Development and In Silico Evaluation of a Model-Based Closed-Loop Fluid Resuscitation Control Algorithm

Xin Jin, Ramin Bighamian, *Member, IEEE*, and Jin-Oh Hahn, *Senior Member, IEEE*

Abstract*—*Objective: **To develop and evaluate in silico, a model-based closed-loop fluid resuscitation control algorithm via blood volume feedback.** ***Methods:*** **A model-based adaptive control algorithm for fluid resuscitation was developed by leveraging a low-order lumped-parameter blood volume dynamics model, and then, in silico evaluated based on a detailed mechanistic model of circulatory physiology. The algorithm operates in two steps: 1) the blood volume dynamics model is individualized based on the patient's fractional blood volume response to an initial fluid bolus via system identification; and 2) an adaptive control law built on the individualized blood volume dynamics model regulates the blood volume of the patient.** ***Results:*** **The algorithm was able to track the blood volume set point as well as accurately estimate and monitor the patient's absolute blood volume level. The algorithm significantly outperformed a population-based proportional-integral-derivative control.** ***Conclusion:*** **Model-based development of closed-loop fluid resuscitation control algorithms may enable the regulation of blood volume and monitoring of absolute blood volume level.** ***Significance:*** **Model-based closed-loop fluid resuscitation algorithm may offer opportunities for standardized and patient-tailored therapy and reduction of clinician workload.**

***Index Terms*—Physiological closed-loop control, semi-adaptive control, system identification, fluid resuscitation, blood volume.**

I. Introduction

FLUID resuscitation refers to therapeutic treatments given to critically ill patients suffering from low blood volume (BV) state, originating from a wide range of pathophysiological conditions such as hemorrhage, infection, and burns [1]–[4]. The ultimate goal of fluid resuscitation is to restore BV deficit in a patient while minimizing undesirable side effects due to fluid overload. Hence, it constitutes a central component in the acute medical management of critically ill patients.

Despite its ultimate goal (i.e., to restore BV deficit), fluid resuscitation in today's clinical arena is performed with the aid of a wide range of endpoints that have been suggested to be adequate surrogates of BV (or fluid responsiveness) in different pathophysiological conditions, since absolute BV level cannot be directly measured. Examples include mean arterial pressure and skeletal muscle oxygen saturation in hemorrhage [5], [6], urinary output in burn injuries [7], and systolic and pulse pressure variability in hypovolemic patients receiving mechanical ventilation [8], [9]. For these reasons, today's fluid resuscitation practice may be susceptible to a large variability in protocol and efficacy, which may in turn increase the cognitive workload of clinicians. Such limitations suggest the potential of closed-loop autonomous fluid resuscitation in standardizing therapy, improving compliance to therapeutic goals, and alleviating clinician workload. In fact, published reports indicate that closed-loop autonomous fluid resuscitation may outperform its manual counterpart in tracking desired endpoint levels by virtue of its vigilance and robustness against disturbances [10]–[12].

However, the vast majority of existing work on closed-loop fluid resuscitation control is largely built upon empirical techniques such as rule base, decision tree, proportional-integral-derivative (PID) control with ad-hoc gain tuning, and fuzzy logic control [5], [7], [10]–[13]. This may be mainly attributed to the absence of mathematical models relevant to rigorous design and analysis of closed-loop fluid resuscitation controllers. Indeed, the majority of existing 1st-principles BV dynamics models developed in the physiology domain [14]–[24] involve excessive details (e.g., ion and protein kinetics as well as complex interaction between extracellular and intracellular compartments), thus leading to formidable sophistications that make these models inadequate for the sake of control design and analysis.

Motivated by the state-of-the-art, the goal of this work was to develop a model-based closed-loop control algorithm for fluid resuscitation, which is able to monitor a patient's absolute BV state accurately. In a series of recent work, we have developed a low-order lumped-parameter model of BV dynamics response to fluid resuscitation [25], [26]. The model takes the form of a simple linear transfer function, while still equipped with critical physiological principles (including intravascular-extravascular compartmental fluid shift [27]) and physiologically relevant parameters (including absolute BV level, inter-compartmental BV

Manuscript received June 7, 2018; revised September 16, 2018 and October 31, 2018; accepted November 8, 2018. Date of publication November 19, 2018; date of current version June 21, 2019. This work was supported in part by the U.S. Office of Naval Research under Grants N000141410591 and N000141512018, and in part by the U.S. National Science Foundation CAREER Award under Grant CNS-1748762. *(Corresponding author: Jin-Oh Hahn.)*

X. Jin is with the Department of Mechanical Engineering, University of Maryland.

R. Bighamian is with the Department of Electrical Engineering, University of Southern California.

J.-O. Hahn is with the Department of Mechanical Engineering, University of Maryland, College Park, MD 20742 USA (e-mail: jhahn12@umd.edu).

Digital Object Identifier 10.1109/TBME.2018.2880927

distribution ratio, and fluid shift rate). By leveraging this model, we develop and rigorously evaluate a closed-loop fluid resuscitation algorithm that operates in two steps: (1) the BV dynamics model is individualized with the patient's fractional BV response to an initial fluid bolus via system identification; and (2) an adaptive control law is built upon the BV dynamics model thus individualized and regulates the BV of the patient. A unique advantage of the algorithm is that it can control the BV of individual patients while at the same time accurately estimate and monitor the patient's absolute BV level. The efficacy of the algorithm was evaluated and analyzed in a wide range of in silico patients created via a detailed cardiovascular circulatory physiology model [28]. To the best of our knowledge, this is the first work that rigorously investigates the model-based development of closed-loop fluid resuscitation controllers.

This paper is organized as follows. Section II presents the architecture of the proposed control algorithm as well as the details of system identification and closed-loop control design. Section III presents the in silico evaluation method employed in this paper. Key results are presented in Section IV and discussed in Section V. Section VI concludes the paper with future work.

II. Model-Based Development of Closed-Loop Fluid Resuscitation Control Algorithm

A. Algorithm Architecture

We propose a two-step adaptive control architecture to cope with the large inter-individual variability in BV dynamics [26]. In this control architecture, the algorithm first individualizes a BV dynamics model to a patient using the patient's fractional BV response (which can be measured in real time by non-invasive blood hemoglobin saturation [29]) to an initial fluid bolus via batch system identification, and second constructs an adaptive control law based on the individualized BV dynamics model (in this context, the BV dynamics model serves as the initial value for subsequent on-line model adaptation), which then regulates BV and monitors absolute BV level (Fig. 1).

The proposed two-step architecture is intended to overcome possible challenges related to the persistent excitation condition (PE) [30] during on-line adaptation of the BV dynamics model. Theoretically, adaptive control algorithm can individualize the BV dynamics model on-line to each patient accurately when the input-output data (fluid infusion-fractional BV response) fulfill the PE condition. However, the fluid infusion profile is determined by therapeutic decisions made for the patient and may thus lack in the PE property to facilitate the on-line adaptation of the BV dynamics model. Thus, the first step of the proposed control architecture (i.e., batch system identification) aims at providing an accurate individualized BV dynamics model that can be leveraged by the second step of the proposed control architecture in constructing an adaptive control algorithm for high-quality BV regulation and absolute BV monitoring. In this way, the individualized BV dynamics model may enhance the quality and performance of the subsequent adaptive control while relaxing its adaptation burden under unpredictable input-output data quality available for on-line adaptive control.

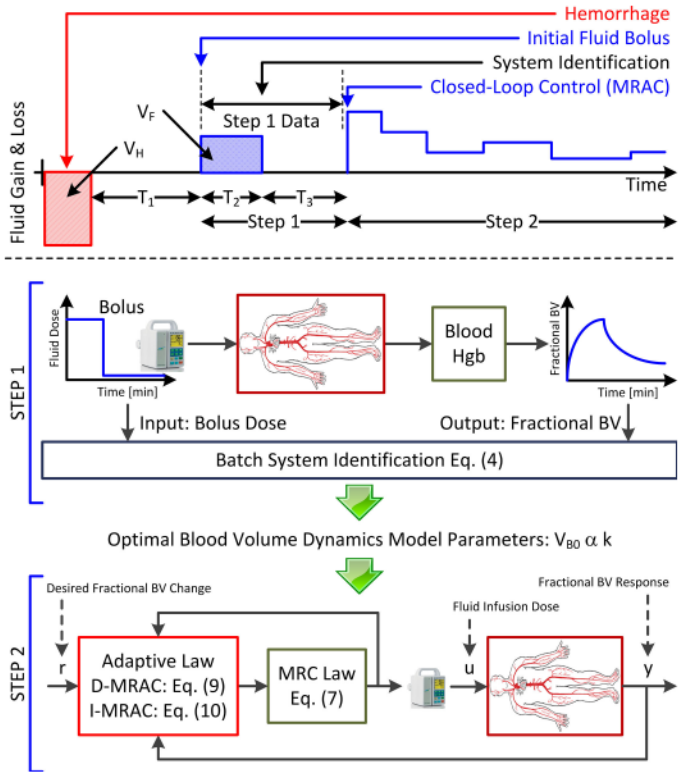

Fig. 1. A two-step control architecture for closed-loop fluid resuscitation algorithm. In the in silico scenario, the patient loses blood (volume: V_H) at $t = 0$. Then, T_1 after blood loss the patient receives an initial fluid bolus (volume: V_F) over the period T_2. Then, T_3 after the bolus batch system identification is performed using the data collected during the period T_2+T_3 ("Step 1 Data") to individualize the blood volume (BV) dynamics model to the patient (STEP 1). Based on the BV dynamics model thus adapted, a model reference adaptive control (MRAC) law is designed. Then, starting from $T_1+T_2+T_3$ after hemorrhage the MRAC initiates operation to regulate BV and monitor absolute BV level (STEP 2). r: reference target (desired fractional BV trajectory). u: control input (fluid infusion dose). y: system output (fractional BV response). V_{B0}, α, and k are the BV dynamics model parameters and represent the absolute BV level, the inter-compartmental BV distribution ratio in the steady-state, and the rate of inter-compartmental fluid shift. Blood Hgb: blood hemoglobin saturation. D-MRAC: direct MRAC. I-MRAC: indirect MRAC.

Further details of these steps are described in the subsections below.

B. Step 1: Batch System Identification

In Step 1, an initial fluid bolus is administered to the patient and the resulting fractional BV response is measured. Then, a batch system identification procedure is performed to adapt a BV dynamics model to the patient with the bolus and fractional BV response as input-output data (Fig. 1).

In our prior work, we developed a lumped-parameter model of BV dynamics response to fluid administration [25], [26]:

$$\ddot{y}(t) + k\dot{y}(t) = \frac{\dot{u}(t)}{V_{B0}} + \frac{ku(t)}{V_{B0}(1+\alpha)} \tag{1}$$

where $y(t) \triangleq \Delta V_B(t)/V_{B0}$ is the fractional (i.e., relative) BV with $\Delta V_B(t)$ the absolute change in BV from its pre-infusion

level V_{B0}, and $u(t)$ is the net positive fluid resuscitation (fluid infusion in excess of urinary output). The fractional BV $y(t)$ is measured via blood hemoglobin saturation [31]:

$$y(t) = \frac{Hgb\,(0) - Hgb(t)}{Hgb(t)} \tag{2}$$

where $Hgb(t)$ [g/dL] is the blood hemoglobin saturation at time t. The model has three parameters equipped with physiological implications: V_{B0} denoting the absolute pre-infusion BV level, α denoting the inter-compartmental BV distribution ratio in the steady state (i.e., the net resuscitated fluid volume is allocated to the blood and interstitial fluid compartments at a 1:α ratio), and k denoting the rate of inter-compartmental fluid shift (the larger k, the more aggressive the fluid shift) [25], [26].

For a given patient, the proposed algorithm individualizes the above BV dynamics model using the measurements of fluid bolus administered to the patient and the patient's fractional BV response. Individualizing the BV dynamics model amounts to determining the parameters V_{B0}, α, and k that best represent the patient's BV dynamics via batch system identification. Noting that the input-output data are discrete, the continuous-time BV dynamics model (1) must be discretized. Invoking the forward Euler approximation for differentiation yields the discrete-time BV dynamics model below:

$$y(i+2) + (kT_s - 2)y(i+1) + (1 - kT_s)y(i) \tag{1}$$

$$= \frac{T_s}{V_{B0}}u(i+1) + \left(\frac{T_s^2 k}{V_{B0}(1+\alpha)} - \frac{T_s}{V_{B0}}\right)u(i) \tag{3}$$

where i is the discrete-time index and T_s is the sampling time. Then, the optimal values of V_{B0}, α, and k associated with the patient are determined by minimizing the discrepancy between the measured fractional BV of the patient (y) and the fractional BV predicted by the discretized BV dynamics model when the fluid bolus data are inputted ($\hat{y}$). This task is fulfilled by solving a numerical optimization problem:

$$\{V_{B0}^*, \alpha^*, k^*\} = \arg \min_{\{V_{B0}, \alpha, k\}} \|y(i) - \hat{y}(i)\| \tag{4}$$

where V_{B0}^*, α^*, and k^* are the optimal parameters that minimize the prediction error norm in (4).

C. Step 2: Adaptive Control With Absolute BV Monitoring

In Step 2, an adaptive control algorithm is constructed using the BV dynamics model individualized to the patient in Step 1. Then, the algorithm regulates the patient's BV and also monitors the patient's absolute BV level by on-line adapting V_{B0}, α, and k with their optimal values obtained in (4) as initial conditions. We employed the model reference adaptive control (MRAC) methodology [32] in constructing the proposed model-based closed-loop control algorithm for fluid resuscitation. Details on the development of the two essential components of MRAC (model reference control (MRC) law and adaptive law) are described in the subsections below.

1) Model Reference Control (MRC) Law Design: In the design of the MRC law, the input u (i.e., fluid infusion) to the BV dynamics model is designed to perfectly track a desired reference trajectory. Taking the Laplace transform of the BV dynamics model yields:

$$y(s) = \frac{1}{V_{B0}}\frac{\left(s + \frac{k}{1+\alpha}\right)}{s\,(s+k)}u(s) = \frac{1}{V_{B0}}\frac{Z_p(s)}{R_p(s)}u(s) \tag{5}$$

where $Z_p(s) = s + \frac{k}{1+\alpha}$ and $R_p(s) = s(s+k)$. Specifying the reference model as the following 1st-order dynamics to achieve a smooth BV change without any overshoot:

$$y_m(s) = \frac{a_m}{s + a_m}r(s) \tag{6}$$

where $a_m > 0$ is the time constant associated with the desired response and r is the reference target (i.e., the desired fractional change in BV), the goal of the MRC law design is to asymptotically drive the output tracking error $e(t) = y(t) - y_m(t)$ to zero. Such a MRC law for the BV dynamics model at hand is given by (see Appendix A for details) [32]:

$$\begin{aligned} \dot{w}_1(t) &= -\lambda w_1(t) + u(t) \\ \dot{w}_2(t) &= -\lambda w_2(t) + y(t) \\ u(t) &= \theta_1 w_1(t) + \theta_2 w_2(t) + \theta_3 y(t) + \theta_4 r(t) \end{aligned} \tag{7}$$

where θ_i, $i = 1, \ldots, 4$ are related to the parameters V_{B0}, α, and k in the BV dynamics model as follows:

$$\begin{aligned} \theta_1 &= \lambda - \frac{k}{1+\alpha} \\ \theta_2 &= V_{B0}(\lambda^2 - \lambda k) \\ \theta_3 &= V_{B0}(k - a_m - \lambda) \\ \theta_4 &= a_m V_{B0} \end{aligned} \tag{8}$$

2) Adaptive Law Design: In MRAC, the parameters in the MRC law are updated either directly (direct MRAC) or indirectly (indirect MRAC). In this study, we considered both direct and indirect MRAC schemes in the development of closed-loop control algorithm for fluid resuscitation. In the direct MRAC, the adaptive law is driven by the output tracking error $e(t) = y(t) - y_m(t)$ to on-line adapt the MRC parameters θ_i, $i = 1, \ldots, 4$ directly [32]:

$$\dot{\hat{\theta}}(t) \triangleq \begin{bmatrix} \dot{\hat{\theta}}_1(t) \\ \dot{\hat{\theta}}_2(t) \\ \dot{\hat{\theta}}_3(t) \\ \dot{\hat{\theta}}_4(t) \end{bmatrix} = -\Gamma_D w(t)\frac{e(t)}{1 + w^T(t)w(t)} \tag{9}$$

where $\hat{\theta}_i(t)$ is the estimate of θ_i at time t, Γ_D is a 4×4 adaptive gain matrix, and $w(t) \triangleq [w_1(t)\ w_2(t)\ y(t)\ r(t)]^T$.

In the indirect MRAC, the adaptive law is driven by the output prediction error $\epsilon(t) = y(t) - \hat{y}(t)$ to on-line adapt the MRC parameters indirectly by first adapting the BV dynamics model parameters and then adapting the MRC parameters based on the relationship (8) [32]. Using the gradient algorithm [32], the

adaptive law is given by (see Appendix B for details):

$$\dot{\hat{\sigma}}(\mathrm{t}) = \Gamma_I \frac{\epsilon(\mathrm{t})}{1+\phi^T(\mathrm{t})\phi(\mathrm{t})}\phi(\mathrm{t}) = \Gamma_I \frac{\mathrm{z}(\mathrm{t}) - \hat{\sigma}^T(\mathrm{t})\phi(\mathrm{t})}{1+\phi^T(\mathrm{t})\phi(\mathrm{t})}\phi(\mathrm{t}) \quad (10)$$

where $\sigma = [\frac{1}{\mathrm{V}_{B0}} \ \frac{\mathrm{k}}{\mathrm{V}_{B0}(1+\alpha)} \ \mathrm{k}]^T$, $\hat{\sigma}(\mathrm{t})$ is its estimate at time t, $\phi(\mathrm{t}) = \mathcal{L}^{-1}\left\{[\frac{\mathrm{su(s)}}{(\mathrm{s}+\lambda_0)^2} \ \frac{\mathrm{u(s)}}{(\mathrm{s}+\lambda_0)^2} \ \frac{-\mathrm{sy(s)}}{(\mathrm{s}+\lambda_0)^2}]^T\right\}$ with $\mathcal{L}^{-1}$ denoting the inverse Laplace transform, $\mathrm{z}(\mathrm{t}) = \mathcal{L}^{-1}\left\{\frac{\epsilon(\mathrm{s})}{(\mathrm{s}+\lambda_0)^2}\right\}$, and Γ_I is a 3×3 adaptive gain matrix. Using $\hat{\sigma}(\mathrm{t})$ thus estimated on-line, the BV dynamics model parameters $\hat{\mathrm{V}}_{B0}(\mathrm{t})$, $\hat{\alpha}(\mathrm{t})$, and $\hat{\mathrm{k}}(\mathrm{t})$ can be estimated. Then, the MRC law can be adapted by updating $\theta_i, \mathrm{i} = 1, \ldots, 4$ according to (8).

D. MRAC Closed-Loop Control of Fluid Resuscitation

Once the MRAC law is constructed as outlined above, the algorithm regulates and monitors the BV of the patient: (1) it regulates the fractional change in BV as dictated by the reference target; and (2) it monitors the absolute BV using the fractional BV measurement and on-line adapted $\hat{\mathrm{V}}_{B0}(\mathrm{t})$:

$$\hat{\mathrm{V}}_B(\mathrm{t}) = \hat{\mathrm{V}}_{B0}(\mathrm{t})\,[1+\mathrm{y}(\mathrm{t})] \quad (11)$$

where $\hat{\mathrm{V}}_B(\mathrm{t})$ is the absolute BV monitored at time t.

III. Methods

The efficacy of the proposed closed-loop control algorithm for fluid resuscitation was evaluated in a wide range of in silico scenarios implemented in MATLAB/SIMULINK environment (MathWorks, Natick, MA). We constructed an in silico patient model based on a well-known comprehensive cardiovascular physiology model [28] and included additional details required for the evaluation of the closed-loop fluid resuscitation control algorithm (Fig. 2). Then, we conducted a rigorous testing of the algorithm while widely varying the physiological state of the in silico patient and the configurable parameters in the in silico scenario shown in Fig. 1. We analyzed the testing results to examine the performance of the batch system identification (Step 1) and MRAC (Step 2) aspects of the two-step control architecture. Details follow.

A. In Silico Patient Model Implementation

We constructed a mathematical model of the patient suited to the in silico testing of the proposed closed-loop fluid resuscitation control algorithm by expanding a circulatory physiology model developed by Guyton [28] (Fig. 2). Then, we created in silico patients by randomly perturbing a subset of key parameters in the model within a physiologically reasonable range.

The model is equipped with essential features related to the BV dynamics and blood pressure regulation, including the circulatory dynamics, interaction between circulatory and interstitial fluid compartments, renal function, sympathetic nerve stimulation, autoregulation, and angiotensin control mechanism, making it an adequate choice for simulating short-term and

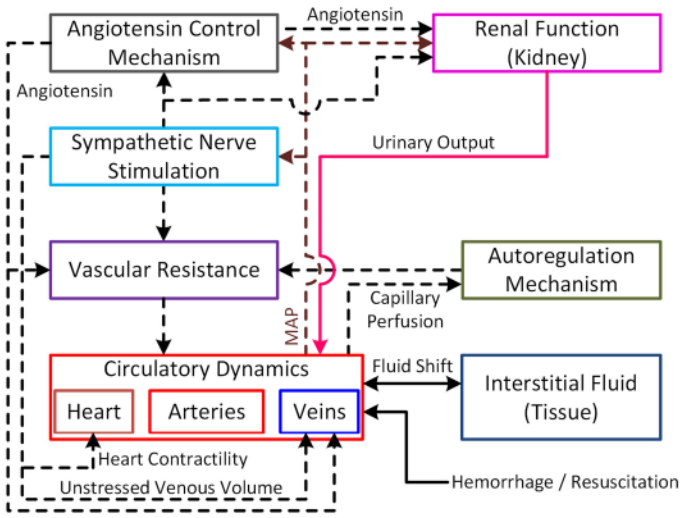

Fig. 2. Patient model for in silico testing of closed-loop fluid resuscitation control algorithm. Solid lines indicate the flow of physical quantity, while dashed lines indicate sensing and actuation.

longer-term regulation of BV, cardiac output, and blood pressure with high fidelity. In this model, the circulatory dynamics represents the BV dynamics in the intravascular space and includes arteries, veins, and the heart as compliant compartments that hold BV. The model is also equipped with the BV modulation by the interstitial fluid and kidneys as well as blood pressure regulation functions including: volume exchange between blood and interstitial fluid via intravascular-extravascular compartmental fluid shift, volume loss due to the urine produced by the renal function in the kidneys, and the modulation of cardiac contractility, vascular resistance, and unstressed venous BV via the sympathetic nerve stimulation driven by blood pressure, autoregulation driven by capillary blood flow, and angiotensin control mechanism.

To facilitate its application to in silico testing of the proposed closed-loop fluid resuscitation control algorithm, two important expansions were made: capability to simulate hemorrhage- and fluid resuscitation-induced BV changes as well as to compute hematocrit, hemoglobin saturation, and fractional BV. The BV changes triggered by hemorrhage and fluid resuscitation was simulated by subtracting and adding volume to the intravascular compartment directly according to the rate of hemorrhage and fluid infusion, respectively. Noting that hemorrhage involves the loss of plasma (PV) and red blood cell (RBCV) volumes, the model was expanded to include separate state variables for PV and RBCV. In particular, the time rate of change in the RBCV was computed as follows:

$$\dot{\mathrm{V}}_{RBC}(\mathrm{t}) = -\mathrm{H}(\mathrm{t})\frac{\mathrm{V}_{RBC}(\mathrm{t})}{\mathrm{V}_B(\mathrm{t})} = -\mathrm{H}(\mathrm{t})\frac{\mathrm{V}_{RBC}(\mathrm{t})}{\mathrm{V}_P(\mathrm{t})+\mathrm{V}_{RBC}(\mathrm{t})} \quad (12)$$

where $\mathrm{V}_P(\mathrm{t})$ and $\mathrm{V}_{RBC}(\mathrm{t})$ are the PV and the RBCV, respectively, and $\mathrm{H}(\mathrm{t})$ is the hemorrhage rate. Using the PV and RBCV, hematocrit $\mathrm{Hct}(\mathrm{t})$ at each time t was computed as $\mathrm{Hct}(\mathrm{t}) = \frac{\mathrm{V}_{RBC}(\mathrm{t})}{\mathrm{V}_P(\mathrm{t})+\mathrm{V}_{RBC}(\mathrm{t})}$, and the hemoglobin saturation

$\mathrm{Hgb(t)}$ was computed as $\mathrm{Hgb(t)} = \frac{1}{3}\mathrm{Hct(t)}$ [33]. Then, the fractional BV was computed using (2).

To conduct in silico testing of the proposed closed-loop fluid resuscitation control algorithm in a wide range of patients, we created 30 in silico patients with wide-ranging physiology by randomly perturbing the key parameters in the patient model up to 40%. These included nominal model parameter values as well as the parameters responsible for the regulation of cardiac contractility, vascular resistance, unstressed venous BV, renal function, and intravascular-extravascular fluid shift. Such a perturbation resulted in a wide range of patients with initial BV level of 3.7∼6.3 L (nominal: 5.0 L) and inter-compartmental BV distribution ratio of 1.7∼3.8 (nominal: 2.3).

B. In Silico Testing Scenario

For each in silico patient created above, the control algorithm was tested in a hemorrhage resuscitation scenario shown in Fig. 1 with a wide range of physiological states as follows.

In the in silico scenario, the patient lost blood (volume: $\mathrm{V_H}$) at $\mathrm{t} = 0$. Then, $\mathrm{T_1}$ after blood loss the patient received an initial fluid bolus (volume: $\mathrm{V_F}$) over the period $\mathrm{T_2}$. Then, $\mathrm{T_3}$ after the bolus batch system identification was performed using the data collected during the period $\mathrm{T_2} + \mathrm{T_3}$ ("Step 1 Data" in Fig. 1) to individualize the BV dynamics model to the patient. Using the BV dynamics model thus adapted, an MRAC adaptive control law was designed based on the BV dynamics model. Then, starting from $\mathrm{T_1} + \mathrm{T_2} + \mathrm{T_3}$ after hemorrhage the MRAC initiated its operation to regulate BV and monitor absolute BV level. To examine the control algorithm rigorously in a wide range of conditions, the configurable parameters (including $\mathrm{V_H}$, $\mathrm{V_F}$, $\mathrm{T_1}$, $\mathrm{T_2}$, and $\mathrm{T_3}$) associated with the in silico scenario were widely varied around nominal values ($\mathrm{V_H} = 2.5\mathrm{L}$, $\mathrm{V_F} = 0.5\mathrm{L}$, $\mathrm{T_1} = 120$ min, $\mathrm{T_2} = 30$ min, $\mathrm{T_3} = 10$ min).

The parameters in the control algorithm were set as follows. The reference target (i.e., the desired fractional change in BV) was set such that BV was resuscitated to pre-hemorrhagic level (it is noted that this reference target was chosen only for testing purposes, though it may not be implementable in real practice). The following MRAC parameters were used in all the in silico testing: $\mathrm{a}_m = 0.067$ (i.e., a reference model time constant of 15 min), $\lambda = 0.4$, $\Gamma_D = \mathrm{I}_{4\times4}$, $\lambda_0 = 0.1$, and $\Gamma_I = \begin{bmatrix} 10 & 0 & 0 \\ 0 & 0.03 & 0 \\ 0 & 0 & 2 \end{bmatrix}$. In particular, the MRAC parameters λ and λ_0 as well as Γ_D and Γ_I were determined by trial and error to achieve adequate set point tracking and on-line parameter estimation performance. A Step 2 period of 80 min was considered in the in silico testing.

To enable realistic in silico evaluation, the control algorithm was implemented digitally with a sampling time of 0.5 min. In addition, simulated fractional BV was contaminated by adding a uniform random noise of sizable magnitude (0.01) to reflect the inaccuracy associated with the blood hemoglobin saturation measurement [34]. To mitigate the adverse impact of noise on the efficacy of the control algorithm, the simulated blood hemoglobin saturation measurement was pre-smoothed via 6-point moving average filtering before employed in the control law computation.

C. In Silico Testing and Data Analysis

In silico testing data were obtained by applying the proposed control algorithm to the 30 randomly created patients. Then, an analysis was conducted to investigate the efficacy of the control algorithm in terms of batch system identification (Step 1) and adaptive control (Step 2). The batch system identification was evaluated by (1) the error between the true versus model-predicted fractional BV, (2) the accuracy of the estimated model parameters, and (3) the variance and covariance properties of the estimated model parameters. The adaptive control was evaluated by its set point tracking and on-line parameter estimation performance.

For each randomly created patient undergoing the in silico testing scenario, the BV dynamics model (1) was individualized by solving the optimization problem (4) based on a Hessian-based algorithm (Levenberg-Marquardt algorithm) in MATLAB with its Optimization Toolbox (MathWorks, Natick, MA) from the initial fluid bolus and fractional BV data during Step 1 period (Fig. 1). Subsequently, the MRAC law was implemented with the individualized BV dynamics model parameters as initial condition for the control and adaptive law parameters. Then, the MRAC was employed to regulate BV and monitor absolute BV.

In evaluating the efficacy of the batch system identification, the root-mean-squared error (RMSE) between the true fractional BV versus the fractional BV predicted by the BV dynamics model in Step 1 period was assessed. In addition, the accuracy of the individualized absolute BV (V_{B0}) and steady-state BV distribution ratio (α) parameters was examined. Furthermore, the reliability of the BV dynamics model parameters was examined via the parametric variance analysis [30]. For this purpose, the discrete-time BV dynamics model (3) was rewritten into the following:

$$\frac{\mathrm{y(i+2)} - 2\mathrm{y(i+1)} + \mathrm{y(i)}}{\mathrm{T}_s^2} = -\mathrm{k}\frac{\mathrm{y(i+1)} - \mathrm{y(i)}}{\mathrm{T}_s} + \frac{1}{\mathrm{V}_{B0}}\frac{\mathrm{u(i+1)} - \mathrm{u(i)}}{\mathrm{T}_s} + \frac{\mathrm{k}}{\mathrm{V}_{B0}(1+\alpha)}\mathrm{u(i)} \tag{13}$$

Then, the variance-covariance matrix associated with the BV dynamics model parameters was computed as follows:

$$\mathrm{Cov}\left(\{\mathrm{V}_{B0}^*, \alpha^*, \mathrm{k}^*\}\right) = \gamma^2 \left[\sum_{\mathrm{i}=1}^{\mathrm{N}} \begin{bmatrix} \frac{\mathrm{d}\ddot{\epsilon}(\mathrm{i})}{\mathrm{dV}_{B0}} \\ \frac{\mathrm{d}\ddot{\epsilon}(\mathrm{i})}{\mathrm{d}\alpha} \\ \frac{\mathrm{d}\ddot{\epsilon}(\mathrm{i})}{\mathrm{dk}} \end{bmatrix} \begin{bmatrix} \frac{\mathrm{d}\ddot{\epsilon}(\mathrm{i})}{\mathrm{dV}_{B0}} & \frac{\mathrm{d}\ddot{\epsilon}(\mathrm{i})}{\mathrm{d}\alpha} & \frac{\mathrm{d}\ddot{\epsilon}(\mathrm{i})}{\mathrm{dk}} \end{bmatrix} \Bigg|_{\{\mathrm{V}_{B0}^*, \alpha^*, \mathrm{k}^*\}} \right]^{-1} \tag{14}$$

where γ is the standard deviation of the output prediction error $\ddot{\epsilon}(\mathrm{k})$. We computed an unbiased estimate of γ as follows [35]:

$$\gamma = \sqrt{\frac{\sum_{\mathrm{i}=1}^{\mathrm{N}} \ddot{\epsilon}^2(\mathrm{i})}{\mathrm{N}}} \tag{15}$$

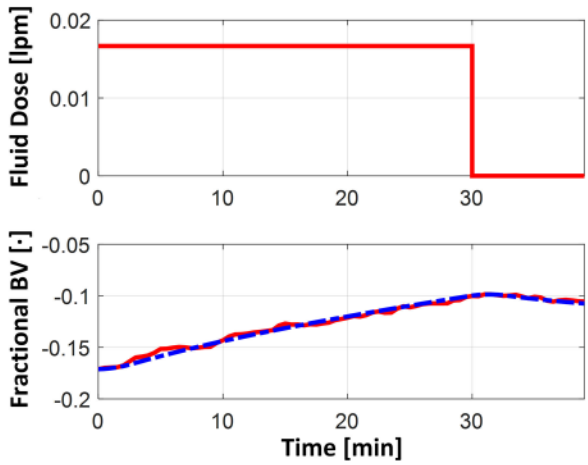

Fig. 3. A representative example of true versus model-predicted fractional BV responses to a fluid bolus. A fluid bolus of 0.5 L (V_F) was given over 30 min (T_2) at a constant infusion rate 120 min (T_1) after 2.5 L blood loss (V_H), followed by a 10 min interval (T_3) before model-reference adaptive control law was constructed and initiated. The resulting 40 min-long data were used for batch system identification to individualize BV dynamics model. Red solid and blue dash dot lines in the bottom plot denote true and model-predicted fractional BV responses, respectively.

The diagonal elements in $\mathrm{Cov}(\{V^*_{B0}, \alpha^*, k^*\})$ denote the variance associated with V^*_{B0}, α^*, and k^*, and the off-diagonal elements indicate the inter-parametric coupling between them. We analyzed all the elements in $\mathrm{Cov}(\{V^*_{B0}, \alpha^*, k^*\})$ to uncover both opportunities and limitations related to the batch system identification in the context of the proposed control algorithm.

In evaluating the efficacy of the MRAC, set point tracking and on-line parameter estimation efficacy was assessed using the in silico data associated with Step 2 period, in terms of percentage error-based (PE) metrics [36] that are widely used in evaluating the computer-driven medication delivery control systems: median PE (MDPE), median absolute PE (MDAPE), divergence, and wobble. To investigate both potential benefits and limitations of the MRAC-based closed-loop fluid resuscitation, we compared its set point tracking and on-line parameter estimation efficacy with two competing alternatives: a proportional-integral-derivative (PID) control, empirically fine-tuned to exhibit comparable set point tracking performance in the nominal in silico patient, and a semi-adaptive MRAC in which α and k are on-line adapted while V_{B0} is fixed at the value individualized by the batch system identification (see Section V for its rationale and details).

The statistical significance in the difference in performance was measured using the paired t-test with MATLAB and its Statistics Toolbox (MathWorks, Natick, MA). The Bonferroni correction was applied in case of multiple comparisons.

IV. Results

Fig. 3 shows a representative in silico example of true versus model-predicted fractional BV responses to a fluid bolus during Step 1 period. In this example, a fluid bolus of 0.5 L (V_F) was given over 30 min (T_2) at a constant infusion rate 120 min (T_1) after 2.5 L blood loss (V_H), followed by a 10 min interval (T_3) before the MRAC law was constructed and initiated. Then, the resulting 40 min-long Step 1 data were used for the batch system identification to individualize the BV dynamics model, and the model-predicted fractional BV response was computed by simulating the BV dynamics model with the fluid bolus. Table I shows the corresponding RMSE as well as the errors and absolute errors (i.e., absolute values of the errors) associated with V_{B0} and α, while Table II shows the normalized median variance and covariance of the BV dynamics model parameters. On the average, the BV dynamics model exhibited $<1\%$ RMSE in reproducing the fractional BV response to a fluid bolus (Fig. 3 and Table I). In addition, the accuracy of the absolute BV level (V_{B0}) individualized by the batch system identification was remarkable (nearly unbiased with $<9\%$ absolute error on the average; Table I). In contrast, the accuracy of the inter-compartmental BV distribution ratio in the steady state (α) was large (40% absolute error on the average with non-trivial bias; Table I). From the variance-covariance analysis, the uncertainty associated with V_{B0} was only $\sim$4.5% of its nominal value, whereas those associated with α and k were $\sim$78% and $\sim$66%, respectively, all in terms of standard deviation (SD; the square root of the variance in Table II). In addition, there was a substantial degree of parametric coupling between α and k.

Fig. 4 shows a representative in silico example of the fractional BV and the resulting mean arterial pressure responses regulated by the direct and indirect MRAC and the population-based PID control during the Step 2 period, in which the control algorithms use noisy fractional BV derived from the blood hemoglobin saturation measurement as feedback in regulating BV and monitoring absolute BV. Table III and Table IV summarize the PE-based metrics obtained from the MRAC and population-based PID control associated with the fractional BV set point tracking (Table III) and on-line parameter estimation (Table IV) errors. All the PE-based metrics associated with the MRACs were significantly superior to the PID control (Table III; indeed, the PID control suffered from larger variability in both fractional BV response and fluid infusion dose than the MRAC in non-nominal in silico patients as

TABLE I
Root-Mean-Squared Errors (RMSEs) in Fractional Blood Volume (BV) and Errors and Absolute Errors Associated With Absolute BV Level (V_{B0}) and Steady-State Inter-Compartmental BV Distribution Ratio (α) Obtained From Batch System Identification of 30 In Silico Patients in Step 1 Period (Mean+/−SD). PE: Percentage Error. PAE: Percentage Absolute Error

	RMSE	V_{B0} Error	α Error
Error	1×10^{-3}+/-3×10^{-4}	0.02+/-0.54 [L]	-0.39+/-1.08
Absolute error		0.43+/-0.32 [L]	0.97+/-0.58
PE [%]	0.8+/-0.3	0.69+/-10.9	-14.0+/-45.5
PAE [%]		8.6+/-6.5	40.1+/-24.6

TABLE II
Normalized Median Variance and Covariance of BV Dynamics Model Parameters Across 30 In Silico Patients in Step 1 Period. Variance and Covariance Values Are Normalized by Respective Nominal Parameter Values Obtained From Batch System Identification

Variance [%]			Covariance [%]		
V_{B0}	α	k	$V_{B0}-\alpha$	$V_{B0}-k$	$\alpha-k$
20.4	6140.3	4375.0	13.8	1.5	-2260.9

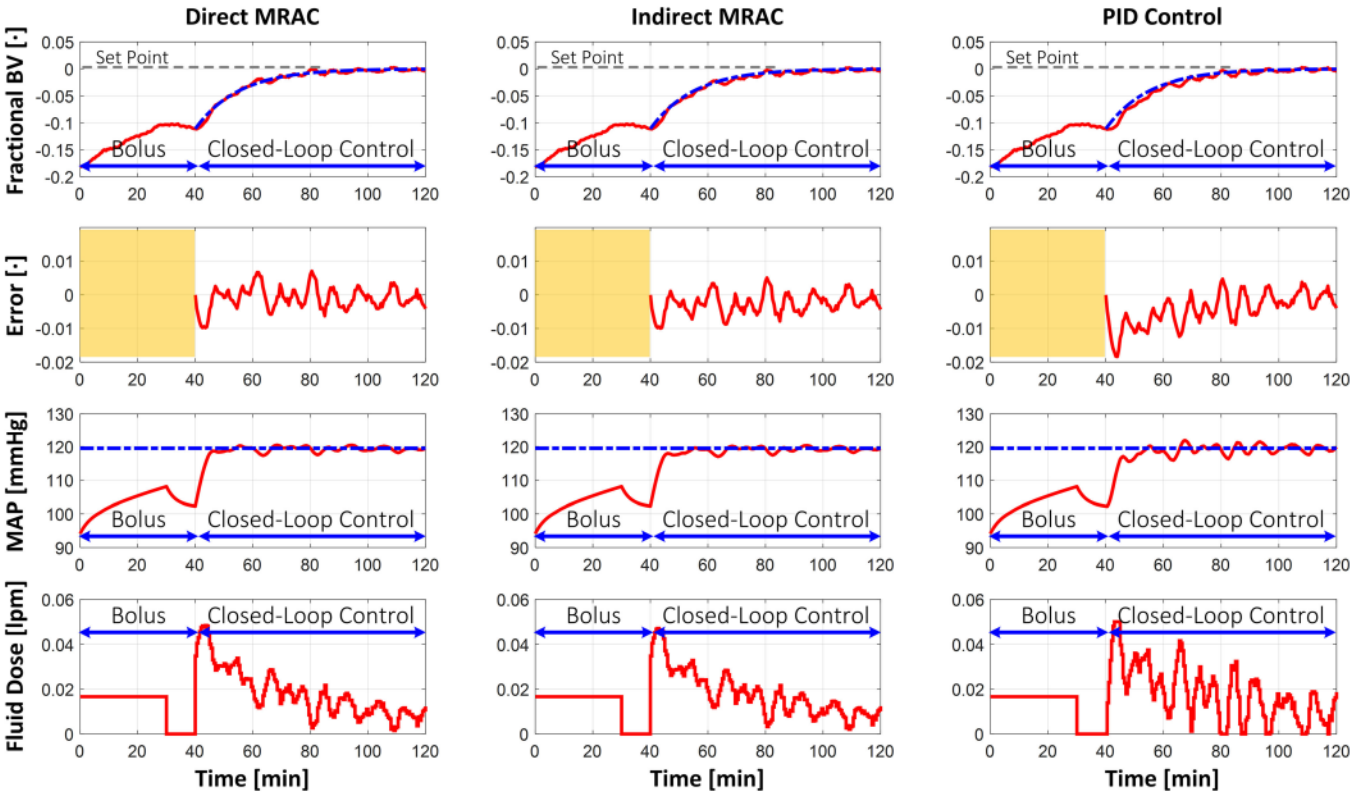

Fig. 4. A representative example of fractional blood volume (BV) and the resulting mean arterial pressure responses regulated by model reference adaptive control (MRAC) and population-based proportionalintegral-derivative (PID) control during Step 2 period, in which control algorithms use noisy fractional BV derived from blood hemoglobin saturation measurement as feedback. Blue dash dot and red solid lines in the top plots denote reference trajectory and actual responses, respectively.

TABLE III
PERCENTAGE ERROR (PE)-BASED METRICS ASSOCIATED WITH FRACTIONAL BLOOD VOLUME (BV) SET POINT TRACKING ERROR OBTAINED FROM MODEL REFERENCE ADAPTIVE CONTROLLERS (MRACS) AND POPULATION-BASED PROPORTIONAL-INTEGRAL-DERIVATIVE (PID) CONTROLLER IN STEP 2 PERIOD (MEAN+/−SD). MDPE: MEDIAN PE. MDAPE: MEDIAN ABSOLUTE PE

	Direct MRAC	Indirect MRAC	PID
MDPE [%]	-7.7+/-3.3†‡	-10.6+/-5.1†	-30.6+/-8.4
MDAPE [%]	16.7+/-4.1†‡	18.9+/-4.0†	34.8+/-8.2
Divergence [%/min]	1.7+/-0.6†‡	1.8+/-0.6†	2.1+/-0.7
Wobble [%]	15.4+/-4.2†	16.3+/-3.5†	20.4+/-5.7

† $p<0.016$ with respect to PID control (paired t-test).
‡ $p<0.016$ with respect to indirect MRAC (paired t-test).

TABLE IV
PERCENTAGE ERROR (PE)-BASED METRICS ASSOCIATED WITH ON-LINE PARAMETER ESTIMATION ERRORS OBTAINED FROM MODEL REFERENCE ADAPTIVE CONTROLLERS (MRACS) IN STEP 2 PERIOD (MEAN+/−SD). MDPE: MEDIAN PE. MDAPE: MEDIAN ABSOLUTE PE

(a) Absolute blood volume (BV) V_{B0}

	Direct MRAC	Indirect MRAC
MDPE [%]	5.5+/-13.3	2.3+/-12.3†
MDAPE [%]	10.0+/-10.3	9.0+/-8.5
Divergence [%/min]	0.02+/-0.09	-0.01+/-0.03†
Wobble [%]	0.6+/-0.5	0.3+/-0.1†

(b) Steady-state inter-compartmental blood volume (BV) distribution ratio α

	Direct MRAC	Indirect MRAC
MDPE [%]	26.3+/-57.7	13.9+/-74.8
MDAPE [%]	43.8+/-46.3	48.8+/-57.8
Divergence [%/min]	0.3+/-1.1	-0.4+/-1.1†
Wobble [%]	11.1+/-7.6	12.2+/-16.0

† $p<0.05$ (paired t-test).

illustrated in Fig. 4). Comparing the direct versus indirect MRAC, the former showed significantly smaller MDPE, MDAPE, and divergence metrics associated with the set point tracking relative to the latter, whereas the latter showed significantly smaller MDPE, divergence, and wobble metrics associated with the on-line estimation of V_{B0} than the former (Table IV(a)). The on-line estimation of α was not satisfactory in both MRAC with non-trivially variable MDPE and MDAPE metrics (Table IV(b)). As far as the mean arterial pressure response was concerned, both the MRAC and the PID control could drive it to the pre-hemorrhagic level: at the end of the Step 2 period, mean arterial pressure resuscitated with the direct and indirect MRAC as well as the PID control reached within 0.9+/−1.0 mmHg, 0.9+/−0.9 mmHg, and 1.1+/−1.2 mmHg of the pre-hemorrhagic level, respectively. In terms of the variability in response (quantified by its standard deviation with respect to the pre-hemorrhagic level over the Step 2 period), the direct and indirect MRAC as well as the PID control yielded 3.5+/−1.5 mmHg, 3.5+/−1.5 mmHg, and 4.2+/−1.5 mmHg, respectively.

Finally, comparing the MRAC versus the semi-adaptive MRAC, all the PE metrics associated with the set point tracking were on the average comparable with statistically insignificant differences of only <7% in direct MRAC and <3% in indirect MRAC.

V. Discussion

Despite the fact that fluid resuscitation intends to restore BV deficit, existing effort on closed-loop fluid resuscitation control has resorted to indirect surrogates of BV. The objective of this study was to systematically develop and evaluate a closed-loop control algorithm for fluid resuscitation based upon direct BV feedback, by leveraging a validated BV dynamics model suited to the design and analysis of control algorithms and monitoring of absolute BV level. Discussed below are the opportunities and limitations of the proposed model-based closed-loop fluid resuscitation control algorithm.

A. Batch System Identification

Our BV dynamics model boasted remarkable performance in reproducing the fractional BV response to fluid bolus as well as estimating the absolute BV level (in terms of V_{B0}) in all the 30 in silico patients. Considering the tremendous degree of structural discrepancy between the in silico testing model versus the BV dynamics model (in the sense that the former is a complex and mechanistic model of circulatory physiology whereas the latter is a low-order lumped-parameter model) as well as the sizable measurement noise, the results strongly illustrate that the BV dynamics model may indeed serve as a viable basis for the development of model-based closed-loop fluid resuscitation control algorithms. Most importantly, it may be possible to realize a closed-loop control algorithm equipped with the ability to monitor absolute BV level, by making use of V_{B0} and on-line fractional BV measurement (as shown in (11)). It must also be emphasized that these observations were robust against wide perturbations in the configurable parameters in the in silico scenario (not shown).

On the other hand, the suboptimal accuracy associated with α may be attributed to two primary reasons. First, α represents steady-state response. Hence, it may be accurately estimated only when the input-output data for the batch system identification includes rich information on the steady state response. Such a limitation can impose a restriction on the input-output data: that data containing predominantly the transient input-output behavior is not suited to quality system identification of the BV dynamics model. To get an estimate of the requisite data length, the value of k (which represents the speed of the BV dynamics) determined for the 30 in silico patients was 0.04 min^{-1} on the average, amounting to an estimated settling time of 100 min. Therefore, the requirement to include steady-state behavior in the input-output data may conflict with the goals of real-world patient care (e.g., it may not be possible to observe a patient for >100 min after a fluid bolus without follow-up fluid therapy). Second, the use of fractional rather than absolute BV as output measurement for system identification may further complicate the issue. According to the BV dynamics model, the fractional BV response to a fluid bolus of magnitude u_0 in the steady-state is $\frac{u_0}{V_{B0}(1+\alpha)}$. Hence, even if the input-output data contains steady-state BV dynamics behavior, the accuracy of α may still be impacted by the accuracy of V_{B0} (which is determined to reproduce both transient and steady-state BV response [25]), i.e., the errors associated with V_{B0} may propagate to α in such a way that the steady-state fractional BV response $\frac{u_0}{V_{B0}(1+\alpha)}$ is still reproduced while the errors in V_{B0} is cancelled by the errors in α.

The variance-covariance analysis could provide additional insights on the opportunities and challenges associated with the batch system identification of the BV dynamics model. In essence, the batch system identification could reliably estimate V_{B0} but not α and k. The unsatisfactory accuracy in α may be attributed to the lack of data representing the steady-state behavior contained in the Step 1 data used in the batch system identification. In turn, the inaccuracy in α propagates to deteriorate the accuracy in k via large the covariance between the two.

In sum, batch system identification with transient fractional BV response data may still be effective in estimating V_{B0} with accuracy, while α and k may suffer from limited accuracy and reliability if sufficient amount of data representing steady-state response are not presented to the system identification.

B. Closed-Loop Fluid Resuscitation Via MRAC

Qualitatively, all the closed-loop control algorithms showed satisfactory set point tracking performance. The fluid infusion dose profile exhibited highly varying trends (consisting of the exponentially decaying trajectory to track the reference model plus high-frequency fluctuation to secure robustness against the noise in the fractional BV measurement), making it challenging to realize such a profile manually by clinicians (unless seriously engaged in the dose adjustment task). It is worth mentioning that manual regulation of BV is not trivial even in the absence of measurement noise. In fact, given that the BV dynamics model is equipped with an integrator, fractional BV increases linearly (i.e., exhibits a ramp response) in response to a constant fluid dose as can be seen in Fig. 3 ($0 < t < 30$ min). However, fractional BV decreases until a steady state is reached due to the fluid shift as soon as the fluid infusion is stopped, as also can be seen in Fig. 3 ($30 < t < 40$ min). These observations strongly illustrate that tight manual regulation of BV can be a challenging task, and therefore, fluid resuscitation may benefit significantly from closed-loop automation.

In terms of set point tracking, both direct and indirect MRAC outperformed the population-based PID control. Comparing the direct versus indirect MRAC, the direct MRAC outperformed its indirect counterpart in set point tracking, while the indirect MRAC showed superior efficacy to its direct counterpart in terms of on-line parameter estimation. These results are intuitively reasonable considering the distinct goals of the on-line parameter estimation in direct versus indirect MRAC: direct MRAC adapts plant model parameters to minimize set point tracking errors while indirect MRAC intends to minimize output prediction errors via on-line parameter estimation.

Sub-optimal performance in the on-line estimation of α may be attributed to the limited PE property in the input-output data as well as to the fact that the adaptive laws in the MRAC do not estimate the BV dynamics model parameters directly. In the direct MRAC, the BV dynamics model parameters are derived from the MRC parameters in (9), which involves solving the nonlinear algebraic equations in (A4) to yield $\mathrm{V}_{B0} = \frac{\theta_2}{\lambda^2 - \lambda \mathrm{k}}$, $\alpha = \frac{\mathrm{k}}{\lambda - \theta_1}$, and $\mathrm{k} = \frac{\theta_2 \mathrm{a}_m + \theta_2 \lambda + \theta_3 \lambda^2}{\theta_2 + \theta_3 \lambda}$. Hence, the inaccuracy in the MRC parameters collectively impact the accuracy of α. In the indirect MRAC, the BV dynamics model parameters are likewise derived from $\hat{\sigma}(\mathrm{t})$ in (10). Noting that $\sigma = [\frac{1}{\mathrm{V}_{B0}} \ \frac{\mathrm{k}}{\mathrm{V}_{B0}(1+\alpha)} \ \mathrm{k}]^T$, V_{B0} and k can be derived from $\hat{\sigma}_1(\mathrm{t})$ and $\hat{\sigma}_3(\mathrm{t})$ directly while α may only be determined from all the elements in $\hat{\sigma}(\mathrm{t})$ (i.e., $\alpha = \frac{\sigma_3}{\sigma_1 \sigma_2} - 1$). Consequently, the errors associated with V_{B0} and k influence the accuracy of α.

The MRAC and PID control were both able to drive the mean arterial pressure back to its pre-hemorrhagic level. Though modest in absolute magnitude, the MRAC still outperformed the PID control in achieving the pre-hemorrhagic mean arterial pressure level, both in accuracy and consistency.

The semi-adaptive MRAC (in which α and k are on-line adapted while V_{B0} is fixed at the value individualized by the batch system identification to optimize the set point tracking task) was motivated by the observation that the benefit of the on-line estimation of V_{B0} by the MRAC's adaptive laws may not be significant. Indeed, the accuracy of the batch versus on-line estimation of V_{B0} was quite comparable (Table I and Table IV) despite the fact that the MRAC adaptive laws leverage V_{B0} individualized from the batch system identification as initial estimate. Hence, it was not surprising that the semi-adaptive MRAC exhibited comparable performance to the standard MRAC in set point tracking.

In summary, main findings from this study are that: adaptive control algorithms for closed-loop fluid resuscitation developed systematically with a low-order lumped-parameter BV dynamics model not only outperformed empiric population-based PID control but also provided a way to monitor absolute BV with adequate accuracy; semi-adaptive MRAC combined with one-time (or alternatively, intermittent) batch estimation of absolute BV level may become a practically viable approach to adaptive closed-loop control of fluid resuscitation; and sub-optimal efficacy of on-line adaptive laws, which may originate from the limited PE property of input-output data (due to, e.g., clinical restrictions related to patient therapy), requires more in-depth investigation on optimizing the overall efficacy of adaptive control strategies to fluid resuscitation.

C. Study Limitation

It is acknowledged that the in silico evaluation scenario used in this paper has limitations in establishing the efficacy of the proposed model-based closed-loop fluid resuscitation control algorithm under a wide range of pathophysiological conditions requiring fluid therapy. In particular, the scenario used in this paper may pertain to only a subset of real-world hemorrhage resuscitation scenarios in which the blood loss is handled early in the therapy, leading to negligible blood loss during the course of fluid resuscitation. In theory, large blood loss during fluid resuscitation may act as a large unknown disturbance that can severely degrade the performance of the algorithm. Moreover, pathophysiological conditions other than hemorrhage (such as infection and burn) are associated with unique alterations in the regulatory mechanisms in the body that were not considered in this paper. Therefore, the evidences collected from this paper must be interpreted as initial proof-of-concept for closed-loop fluid resuscitation control, while much follow-up work must be conducted before its feasibility, efficacy, and limitations can be thoroughly established and elucidated against a wide range of real-world hypovolemic scenarios. A conceivable initial step toward such comprehensive development of closed-loop fluid resuscitation control algorithms may be to expand the BV dynamics model (1) to capture and accommodate a variety of pathophysiology invoking hypovolemia and to exploit such a model as basis for the development and analysis of versatile closed-loop fluid resuscitation control algorithms.

VI. Conclusion

This paper presented a systematic development of innovative closed-loop control algorithms for fluid resuscitation via direct BV feedback. MRAC equipped with the capability for absolute BV estimation and monitoring was developed by leveraging a low-order lumped-parameter BV dynamics model. Rigorous in silico testing with a detailed mechanistic circulatory physiology model elucidated both opportunity for the next generation of fluid resuscitation with patient-specific absolute BV monitoring, as well as challenges associated with the on-line parameter estimation in real-world clinical scenarios.

Future effort must be invested to more rigorous development, analysis, and in silico testing of model-based closed-loop fluid resuscitation control algorithms for various pathophysiological conditions, followed ultimately by experimental investigations to verify the in vivo efficacy of such algorithms and its benefit on clinical outcomes.

Appendix A
Model Reference Control Law Design

Given the plant (i.e., BV dynamics) model and the reference model, consider the following feedback control law [32]:

$$\mathrm{u}(\mathrm{s}) = \frac{\theta_1}{\mathrm{s}+\lambda}\mathrm{u}(\mathrm{s}) + \frac{\theta_2}{\mathrm{s}+\lambda}\mathrm{y}(\mathrm{s}) + \theta_3 \mathrm{y}(\mathrm{s}) + \theta_4 \mathrm{r}(\mathrm{s}) \qquad \text{(A1)}$$

where $\lambda > 0$. Substituting (A1) into the BV dynamics model yields the following closed-loop transfer function:

$$\mathrm{y}(\mathrm{s}) = \frac{\theta_4 \mathrm{Z}_p(\mathrm{s})\,(\mathrm{s}+\lambda)}{[((\mathrm{s}+\lambda)-\theta_1)\,\mathrm{V}_{B0}\mathrm{R}_p(\mathrm{s}) - \mathrm{Z}_p(\mathrm{s})\,(\theta_2 + \theta_3\,(\mathrm{s}+\lambda))]}\mathrm{r}(\mathrm{s}) \qquad \text{(A2)}$$

For perfect model reference tracking, the transfer function (A2) must be equal to the reference model:

$$\frac{\theta_4 \mathrm{Z}_p(\mathrm{s})\,(\mathrm{s}+\lambda)}{[(\mathrm{s}+\lambda-\theta_1)\,\mathrm{V}_{B0}\mathrm{R}_p(\mathrm{s}) - \mathrm{Z}_p(\mathrm{s})\,(\theta_2 + \theta_3\,(\mathrm{s}+\lambda))]} = \frac{\mathrm{a}_m}{\mathrm{s}+\mathrm{a}_m} \qquad \text{(A3)}$$

Solving (A3) for the control law parameters θ_i, $\mathrm{i} = 1, \ldots, 4$ yields the following set of algebraic equations:

$$\begin{aligned}
&\theta_4 = a_m \mathrm{V}_{B0} \\
&\mathrm{V}_{B0}\theta_1 + \theta_3 = \mathrm{V}_{B0}\left(\frac{\alpha \mathrm{k}}{1+\alpha} - \mathrm{a}_m\right) \\
&\mathrm{kV}_{B0}\theta_1 + \theta_2 + \left(\lambda + \frac{\mathrm{k}}{1+\alpha}\right)\theta_3 \\
&\quad = \frac{\alpha \mathrm{kV}_{B0}\lambda}{1+\alpha} - \mathrm{a}_m \mathrm{V}_{B0}\left(\lambda + \frac{\mathrm{k}}{1+\alpha}\right) \\
&\theta_2 + \lambda\theta_3 = -\mathrm{a}_m \mathrm{V}_{B0}\lambda
\end{aligned} \tag{A4}$$

Solving (A4) yields (8), which, together with (A1), constitutes the MRC law. The MRC law, when implemented in the time domain, becomes (7).

Appendix B
Indirect Adaptive Law Design

The BV dynamics model is reformulated into the following linear parametric model:

$$\begin{aligned}
\mathrm{z(s)} &= \frac{\mathrm{s}^2}{(\mathrm{s}+\lambda_0)^2}\mathrm{y(s)} = \sigma^T \phi(\mathrm{s}) \\
&= \left[\begin{array}{ccc} \frac{1}{\mathrm{V}_{B0}} & \frac{\mathrm{k}}{\mathrm{V}_{B0}(1+\alpha)} & \mathrm{k} \end{array}\right] \left[\begin{array}{c} \frac{\mathrm{su(s)}}{(\mathrm{s}+\lambda_0)^2} \\ \frac{\mathrm{u(s)}}{(\mathrm{s}+\lambda_0)^2} \\ \frac{-\mathrm{sy(s)}}{(\mathrm{s}+\lambda_0)^2} \end{array}\right]
\end{aligned} \tag{B1}$$

where $\frac{1}{(\mathrm{s}+\lambda_0)^2}$ with $\lambda_0 > 0$ is a stable filtering included to avoid numerical differentiation. Based on the gradient algorithm, the indirect adaptive law is given by:

$$\begin{aligned}
\dot{\hat{\sigma}}(\mathrm{t}) &= \Gamma_I \frac{\epsilon(t)}{1+\phi^T(\mathrm{t})\phi(\mathrm{t})}\phi(\mathrm{t}) \\
&= \Gamma_I \frac{\mathrm{z}(t) - \hat{\sigma}^T(\mathrm{t})\phi(\mathrm{t})}{1+\phi^T(\mathrm{t})\phi(\mathrm{t})}\phi(\mathrm{t})
\end{aligned} \tag{B2}$$

References

[1] A. Bortolani *et al.*, "Fluid replacement in burned patients," *Acta chirurgiae plasticae*, vol. 38, no. 4, pp. 132–136, 1996.

[2] E. C. Rackow *et al.*, "Fluid resuscitation in circulatory shock: A comparison of the cardiorespiratory effects of albumin, hetastarch, and saline solutions in patients with hypovolemic and septic shock," *Crit. Care Med.*, vol. 11, no. 11, pp. 839–850, 1983.

[3] P. Perel *et al.*, "Colloids versus crystalloids for fluid resuscitation in critically ill patients," *Cochrane Database Syst. Rev.*, vol. 2, 2013, Art. no. CD000567.

[4] J.-L. Vincent and H. Gerlach, "Fluid resuscitation in severe sepsis and septic shock: An evidence-based review," *Crit. Care Med.*, vol. 32, no. 11 Suppl, pp. S451–S454, 2004.

[5] G. C. Kramer *et al.*, "Closed-loop control of fluid therapy for treatment of hypovolemia," *J. Trauma*, vol. 64, no. 4, pp. S333–S341, 2008.

[6] N. F. Chaisson *et al.*, "Near-infrared spectroscopy-guided closed-loop resuscitation of hemorrhage," *J. Trauma*, vol. 54, no. 5 Suppl, pp. S183–S192, 2003.

[7] J. Salinas *et al.*, "Closed-loop and decision-assist resuscitation of burn patients," *J. Trauma*, vol. 64, no. 4 Suppl, pp. S321–S332, 2008.

[8] K. Bendjelid and J. A. Romand, "Fluid responsiveness in mechanically ventilated patients: A review of indices used in intensive care," *Intensive Care Med.*, vol. 29, no. 3, pp. 352–360, 2003.

[9] J. Rinehart *et al.*, "Evaluation of a novel closed-loop fluid-administration system based on dynamic predictors of fluid responsiveness: An in silico simulation study," *Crit. Care*, vol. 15, no. 6, p. R278, 2011.

[10] J. Rinehart *et al.*, "Closed-loop fluid administration compared to anesthesiologist management for hemodynamic optimization and resuscitation during surgery: An in vivo study," *Anesthesia Analgesia*, vol. 117, no. 5, pp. 1119–1129, 2013.

[11] J. Rinehart *et al.*, "Closed-loop assisted versus manual goal-directed fluid therapy during high-risk abdominal surgery: A case-control study with propensity matching," *Crit. Care*, vol. 19, no. 1, pp. 1–11, 2015.

[12] J. Rinehart *et al.*, "Intraoperative stroke volume optimization using stroke volume, arterial pressure, and heart rate: Closed-loop (learning intravenous resuscitator) versus anesthesiologists," *J. Cardiothoracic Vasc. Anesthesia*, vol. 26, no. 5, pp. 933–939, 2012.

[13] N. R. Marques *et al.*, "Automated closed-loop resuscitation of multiple hemorrhages: A comparison between fuzzy logic and decision table controllers in a sheep model," *Disaster Mil. Med.*, vol. 3, no. 1, pp. 1–10, 2017.

[14] T. Tatara and C. Tashiro, "Quantitative analysis of fluid balance during abdominal surgery," *Anesthesia Analgesia*, vol. 104, no. 2, pp. 347–354, 2007.

[15] T. Tatara *et al.*, "Crystalloid infusion rate during fluid resuscitation from acute haemorrhage," *Brit. J. Anesthesia*, vol. 99, no. 2, pp. 212–217, 2007.

[16] D. E. Carlson *et al.*, "Impairment of blood volume restitution after large hemorrhage: A mathematical model," *Amer. J. Physiol.*, vol. 270, pp. R1163–R1177, 1996.

[17] C. C. Gyenge *et al.*, "Preliminary model of fluid and solute distribution and transport during hemorrhage," *Ann. Biomed. Eng.*, vol. 31, pp. 823–839, 2003.

[18] G. Arturson *et al.*, "Computer simulation of fluid resuscitation in trauma: First pragmatic validation in thermal injury," *J. Burn Care Res.*, vol. 10, no. 4, pp. 292–299, 1989.

[19] A. L. Cervera and G. Moss, "Crystalloid distribution following hemorrhage and hemodilution: Mathematical model and prediction of optimum volumes for equilibration at normovolemia," *J. Trauma Acute Care Surg.*, vol. 14, no. 6, pp. 506–520, 1974.

[20] J. C. Pirkle and D. S. Gann, "Restitution of blood volume after hemorrhage: Mathematical description," *Amer. J. Physiol.*, vol. 228, no. 2, pp. 821–827, 1975.

[21] A. Hedlund *et al.*, "Computer simulation of fluid resuscitation in trauma. I. Description of an extensive pathophysiological model and its first validation," *Comput. Methods Programs Biomed.*, vol. 27. pp. 7–21, 1988.

[22] J. Kofránek and J. Rusz, "Restoration of Guyton's diagram for regulation of the circulation as a basis for quantitative physiological model development," *Physiol. Res.*, vol. 59, pp. 897–908, 2010.

[23] J. C. Pirkle and D. S. Gann, "Mathematical model of blood volume control after hemorrhage: Implication for intravenous fluid therapy," *Proc. Summer Comp. Sim. Conf.*, pp. 482–485, 1976.

[24] M. C. Mazzoni *et al.*, "Dynamic fluid redistribution in hyperosmotic resuscitation of hypovolemic hemorrhage," *Amer. J. Physiol.*, vol. 255, pp. H629–H637, 1988.

[25] R. Bighamian *et al.*, "A lumped-parameter subject-specific model of blood volume response to fluid infusion," *Front. Physiol.*, vol. 7, p. 390, 2016.

[26] R. Bighamian *et al.*, "In-human subject-specific evaluation of a control-theoretic plasma volume regulation model," *Comput. Biol. Med.*, vol. 91, pp. 96–102, 2017.

[27] A. C. Guyton *et al.*, *Dynamics and Control of Body Fluid*. Philadelphia, PA, USA: W.B. Saunders Company, 1975.

[28] A. C. Guyton, *Circulatory Physiology III: Arterial Pressure and Hypertension*. Philadelphia, PA, USA: W.B. Saunders Company, 1980.

[29] D. Frasca *et al.*, "Accuracy of a continuous noninvasive hemoglobin monitor in intensive care unit patients," *Crit. Care Med.*, vol. 39, no. 10, pp. 2277–2282, Oct. 2011.

[30] L. Ljung, *System Identification: Theory for the User*, 2nd ed. Upper Saddle River, NJ, USA: Prentice-Hall, 1999.

[31] R. G. Hahn, "Volume kinetics for infusion fluids," *Anesthesiology*, vol. 113, no. 2, pp. 470–481, 2010.

[32] P. A. Ioannou *et al.*, *Robust Adaptive Control*. Upper Saddle River, NJ, USA: Prentice-Hall, 1996.

[33] S. M. Lewis *et al.*, *Dacie and Lewis's Practical Haematology*, 9th ed. Edinburgh, U.K.: Churchill Livingstone, 2001.

[34] C. Bergek *et al.*, "Accuracy of noninvasive haemoglobin measurement by pulse oximetry depends on the type of infusion fluid," *Eur. J. Anaesthesiol.*, vol. 30, no. 2, pp. 73–79, 2013.

[35] K. J. Keesman, *System Identification—An Introduction*. London, U.K.: Springer-Verlag, 2011.

[36] J. R. Varvel *et al.*, "Measuring the predictive performance of computer-controlled infusion pumps," *J. Pharmacokinetics Biopharmaceutics*, vol. 20, no. 1, pp. 63–94, 1992.